RSC Advances

PAPER

View Article Online
View Journal | View Issue

Cite this: *RSC Adv.*, 2015, **5**, 13653

Nanotexturing of PC/n-HA nanocomposites by innovative and advanced spray system

Barnali S. Banerjee and K. Balasubramanian*

Nanoscale texturing of a nano-hydroxyapatite (n-HA) filler on a polycarbonate (PC) matrix is ameliorated by advanced engineered spray techniques *viz.* spray gun and centrifuged spray drying, concerned with modifying topographical properties for biomedical grade screw/plate coating application. Mathematical evaluation of the factors affecting the texture of the thin film PC/n-HA nanocomposite has been modelled for the centrifuged spray dryer concerning homogeneity and symmetric dispersion of n-HA pitching on the PC medium. FTIR illustrates the functional group vibration peaks of 1093 cm^{-1} and 603 cm^{-1} of PC/n-HA nanocomposites due to the presence of PO_4^{3-}. XRD infers the average crystal size of n-HA ≤20 nm in the PC/n-HA nanocomposite, which possesses consistency in the FESEM micrograph, confirming the various dispersion comparisons between spray gun film and centrifuged spray dried film. Topographical analysis of PC/n-HA film acquired by the two modes of spraying exemplifies surface roughness of 81.4 nm by the spray gun and 132 nm by the centrifuged spray dryer technique, with increasing spikes affirming the uniform scaffold structure of the n-HA embedment over the PC medium, thus, providing the hydrophobic trait needed for corrosion resistant application. Contact angle analysis shows the wettability and adhesive property of the PC/n-HA nanocomposite and delivers a 131.7° contact angle for innovative centrifuged spray dryer technique. Hence, the modelled parameters emphasize the applicability of the innovative designed centrifuged spray dryer technique for biomedical coating applications.

Received 29th November 2014
Accepted 23rd December 2014

DOI: 10.1039/c4ra15488f

www.rsc.org/advances

1. Introduction

An innovative approach for the repair and regeneration of tissues and organs deliver a high impact over commercial regenerative medicine era consisting of cells and constituents. Conventional orthopaedic implants designed have been relatively effective, but the necessity to improve their long-term functionality remains. For example, typical fabrication using metals, such as stainless steel (SS), titanium alloy, and cobalt–chromium alloys, are expedient for conventional knee and hip implants. To enhance the amalgamation of inherent tissue, bone-contacting surfaces are usually encapsulated with calcium phosphates for the osteoinductive process.[1]

Nano-hydroxyapatite (n-HA) is a well scrutinized biocompatible inorganic mineral that exemplifies intrinsic bone mimicking characteristics for encouraging osteo-development. Moreover, better amalgamated bioactivity can be achieved by increasing the content of HA filler.[2] However, for bone apposition to HA-coated implants, few disputes are hovering over the difficulties regarding structural and chemical features of coated implantation and calcium phosphate.[3] Moreover, glitches, which affect the long-term enactment of the implantation scheme, involve sterile slackening due to insertions, mismatching in mechanical characteristics, stress-shielding and osteo-resorption, oxidization and fatigue failure, provocative reactions to particulate wear fragments and other processing inadequacies,[4,5] whereas polycarbonate (PC), a potential commercialized based engineering thermoplastic, possesses severe typical properties, including wetness insensitivity, high thermal distortion temperature, dimensional constancy and flame resistance.[6] A few studies have been reported on the subsequent weakening in mechanical properties of chitosan/HA biocomposites comprising nano-sized HA particles.[7] Several reports and investigations documented the incorporation of n-HA fillers in a PC matrix that enhances the automated mechanical characteristics of the PC/n-HA composite as compared to the individual constituents.[8,9] Innate osteo-matrix is, in fact, an animate/inanimate complex substantial.[10] Therefore, for the reinforcement of bone tissue, a substantial complex composed of PC/n-HA is favourable as a scaffolding material.

In the view of the abovementioned validation, the present work deals with tailoring the nano texture of a PC/n-HA composite by two advanced differentiable techniques of spraying film modification that includes the spray gun and the centrifuged spray dryer technique, both featuring a distinctive configuration of molecular laminar bedding pattern for

Department of Materials Engineering, DIAT (DU), Ministry of Defence, Girinagar, Pune, Maharashtra, India. E-mail: meetkbs@gmail.com; Fax: +91-020-2438-9509; Tel: +91-020-2438-9680

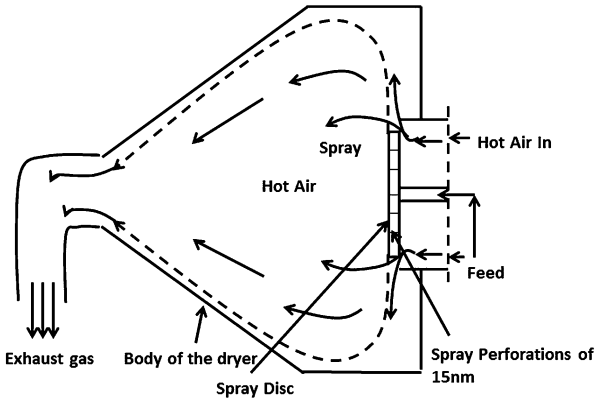

Fig. 1 Flow of feed and hot air through centrifuged spray dryer.

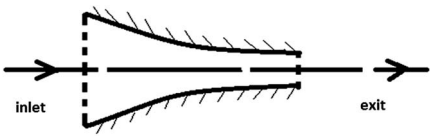

Fig. 2 Steady state steady flow outline at nozzle tip.

advancement in osteointegration system. Distinctive properties of the spray gun method and centrifuged spray dryer are given in Table 1.[11–13]

2. Materials and methods

The polycarbonate (PC) used in this study was supplied by SABIC Innovative Plastics India Pvt. Ltd. under the trade name LEXAN 143R. Nano hydroxyapatite (n-HA) was procured from Sigma Aldrich Chemicals Pvt. Ltd, USA. All the chemicals were used as received without any treatment.

In an exemplary synthesis approach, the particulate composite thin film of individual samples of 30, 60, or 80 wt% of PC/n-HA was prepared by a spray coating method. Modification in thin film of PC/n-HA is performed by proper dispersion of n-HA in the PC matrix by running a batch reaction on an ultrasonication probe (20–40 kHz) with a power of 750 W for 8 hours. Furthermore, the PC/n-HA thin film was acquired by applying a spray system onto the glass slide, first with the aid of a spray gun and then with a centrifuged spray dryer at the optimized concentration of 80 wt% of PC/n-HA. A Brookfield DV-E Viscometer (Brookfield Engineering Laboratories, Inc, USA) was used to measure the viscosity of the composite solution at 25 °C and 80% R.H. at 100 rpm.

2.1 Characterization

The FTIR spectrum was recorded and compared for pristine PC and n-HA, as well as for the PC/n-HA film. The spectrum was chronicled between 3000 and 500 cm^{-1} with KBr pellets at room temperature using a PerkinElmer Spectrum BX FTIR system (PerkinElmer Inc., USA). XRD analysis of n-HA and PC/n-HA was carried out using a Bruker AXS D8 (U.S.A) Advanced diffractometer with Cu Kα radiation. The surface morphologies of thin film samples from the two different modes of spraying techniques were examined using FESEM Imaging, obtained using a Carl Zeiss field emission scanning electron microscope (Carl Zeiss AG, Germany). The hydrophobic trends of the PC/n-HA films for comparative studies of the spray techniques were monitored by a KRÜSS Drop Shape Analyser, DSA25 (Germany) and successive topographic analysis of samples were observed using AFM (Asylum Research, an Oxford instrument company, UK) in tapping mode.

2.2 Designed mechanism of centrifuged spray dryer

Solutions can be dried by spraying them as fine droplets into a stream of hot gas in a centrifuged spray dryer. The solution to be dried is introduced into the drying chamber, where the droplets are dispersed into the stream of heated air. A drop of liquid reaches its terminal velocity in the gas stream within inches of the spraying nozzle and evaporation simultaneously takes place at the surface of the drop. Rapid drying occurs due to evaporation of liquid from particles inside the spray chamber. To obtain rapid drying, the solution is sprayed to provide small particles of high surface/weight ratios, whose diameters are usually in the range of 10–60 μm. For the same purpose, the spray nozzle bears a rotating disc that permits even distribution of particles with moderate variation in liquid flow rate and without change in droplet size.[11]

Accounting for the pros of the continuous drying method at an industrial scale using the centrifuged spray dryer, the present study deals with the modelling of a laboratory scale process in designing the centrifuged spray dryer in which a PC/

Table 1 Comparison between spray gun and centrifuged spray gun mechanism

Spray gun	Centrifuged spray dryer
1. Elongation in drying time interval	1. Instantaneous drying technique
2. Spray nozzle gives a liquid stream comprised of droplets of sizes more than 50 μm	2. Centrifugal nozzle breaks the liquid stream into enormous droplets of size of 10–15 nm
3. No rotary spray disc is provided on spray gun nozzle tip	3. Distribution of particle size about the mean of spray disc is fairly constant
4. Spray nozzle flow rate is low	4. Solid cone nozzle of centrifuged spray dryer provides high jet impact and correspondingly higher flow rate.
5. Less pressure drop across nozzle	5. Greater pressure drop across the nozzle orifice produces smaller droplets

n-HA solution is dispersed into a stream of hot gas in the form of a mist of fine droplets. The droplets are sprayed inside a cylindrical drying chamber by a pressure nozzle attached to a spray disk consisting of numerous perforations of 10–15 nm diameters for the uniform jet impact of droplets on the glass slide. Moisture gets rapidly vaporized from the droplets, leaving the residual particle as the dry thin film. The flow of gas and solution sprayed may be concurrent, countercurrent or a combination of both.[12] The advanced spraying device in the experiment is devised with a rotary disc equipped with a solid cone spray nozzle for providing centrifugal force to the PC/n-HA solution. A solid cone nozzle spray is usually employed for uniform particle diffusion and is equipped with a rotating disc that provides increased flow rate of spraying. The included angle of the solid cone nozzle is nearly equal to 30°–100° and allows the variation in flow rate of 3–8 μl s^{-1}.[13] The accessible parameters for the centrifuged spray drying technique were modelled to account for factors affecting the texture of the thin PC/n-HA film and can be enormously illustrated by Fig. 1 and 2.

2.3 Evaluation of texture-affecting parameters

2.3.1 Flow past single sphere. For the evaluation of heat transfer between a flowing fluid and the surface of a single sphere, the heat transfer coefficient for an individual drop coming out of the solid cone nozzle of the centrifuged spray dyer can be described as follows:

$$\frac{hD_p}{k_f} = 2.0 + 0.60\left(\frac{D_pG}{\mu_f}\right)^{0.5}\left(\frac{C_p\mu_f}{k_f}\right)^{1/3} \quad (1)$$

where D_p is the diameter of a spherical drop, estimated for the spray dryer as the volume–surface mean diameter D_s of drops from the spray disk, given by[12]

$$D_s = 12.2 \times 10^4 r\left(\frac{M}{\rho_l n r^2}\right)^{0.6}\left(\frac{\mu}{M}\right)^{0.2} \quad (2)$$

where, D_s = average drop diameter (nm), For the PC/n-HA system, the calculated data for eqn (2) parameters are given as, r = spray disk radius, 1.2 cm, M = spray mass rate per length of disk periphery = $\rho av/l = 4.2 \times 10^8$ g cm^{-1} s^{-1}, ρ = density of solution, 0.8 g cm^{-3}, n = disk speed, 500–600 r per min, μ = viscosity of liquid, 27 cP (measured by Brookfield DV-E Viscometer at 25 °C, 80% R.H., and 100 rpm), L_p = disk periphery, $2\pi r = 7.536$ cm, Assuming the surface tension of PC/n-HA nanocomposite (ref. ACCU DYNE TEST™ chart for polymers), σ = surface tension of PC/n-HA solution, 52 000 g s^{-2}.

Thus, by substituting the values of the respective parameters of eqn (2), the average drop diameter from spray dryer can be calculated as

$$D_s = 12.2 \times 10^4 r\left(\frac{M}{\rho_l n r^2}\right)^{0.6}\left(\frac{\mu}{M}\right)^{0.2}\left(\frac{\sigma\rho_l L_p}{M^2}\right)^{0.1} = 48.28 \times 10^{-7} \text{ m}$$

2.3.2 Velocity and impact of jet spray. The impact of the jet spray coming out of the pressure nozzle on the stationary vertical plate attributes to the homogeneity of the n-HA filler over the PC matrix and the uniformity in texture can be given as follows:[14]

$$F_x = \rho a V^2 \quad (3)$$

where, F_x = rate of change in momentum in the direction of force, ρaV = rate of mass sprayed, V = velocity of jet.

At the tip of the pressure nozzle, assuming a steady state steady flow equation,

$$h_i + \frac{v_i^2}{2} + gz_i + q = h_e + \frac{v_i^2}{2} + gz_e + w \quad (4)$$

v_i, gz_i, q, gz_e, $w = 0$ (negligible).

The velocity of the jet can be given as

$$v_e = \sqrt{2(h_i - h_e)} \quad (5)$$

where h is the enthalpy of the system.

Accounting for the theoretical data, experimentation on the centrifuged spray dryer contributes the pressure drop of 5.9 kg cm^{-2} at the tip of nozzle, thus the velocity of the PC/n-HA jet can be deliberated as

$$v_e = \sqrt{2g_c\Delta P/\rho} = \sqrt{2 \times 9.81 \times 5.9/0.8} = 38.03 \text{ m s}^{-1} \quad (6)$$

where g_c is the acceleration due to gravity. ΔP is the difference in pressure head at the inlet and outlet of the nozzle.

The impact of the jet spray coming out of the pressure nozzle is calculated as

$$F_x = \rho a v_e^2 = 800 \times 4.5 \times 10^{-4} \times (38.03)^2 = 520.66 \text{ N} \quad (7)$$

3. Results and discussion

3.1 IR analysis

The surface and dispersion properties of the PC/n-HA film at optimized loading of 80 wt% have been investigated by significant characterization tools for biomedical grade screw/plates coated with engineering modified PC/n-HA nano composite concerning osteointegration process. Fig. 3 shows IR spectra of

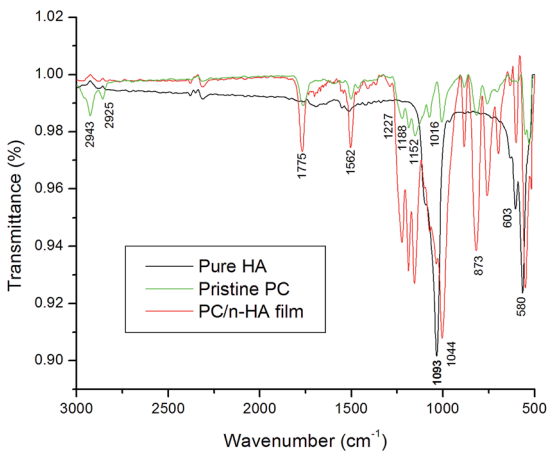

Fig. 3 IR spectra of (a) pure HA (b) pristine PC (c) PC/n-HA film.

pure HA, pristine PC and PC/n-HA film, determining the comprised functional groups.

It can be observed that the characteristic peaks of n-HA and PC deviate slightly in the PC/n-HA film, which shows C–O stretching vibration peaks at 1776 cm^{-1} and 1562 cm^{-1}, whereas the signature crests in PC characterize an intense triplet of 1152, 1188 and 1227 cm^{-1}.[15] The characteristic peak at 1772 cm^{-1} is due to the carbonyl C=O stretch, and the strongest infrared absorptions in PC are due to the C–O single bond stretches that continue down to 1000 cm^{-1}, with the strongest of these at 1016 cm^{-1}.[6,16] The peak at 2943 cm^{-1} of pristine PC belongs to the asymmetric stretching vibration, which moves to 2925 cm^{-1} in the thin film PC/n-HA composite. For HA, the peaks at 3672 cm^{-1} and 580 cm^{-1} belong to the stretching vibration of the hydroxyl group (–OH),[17,18] whereas the peaks at 1093 cm^{-1} and 603 cm^{-1} belong to PO_4^{3-}.[19] In the composite, the peak at 873 cm^{-1} of n-HA crystal was attributed to HPO_4^{2-}, and the peak of PO_4^{3} at 1093.35 cm^{-1} of n-HA crystal moves to 1044 cm^{-1}.[20]

3.2 XRD analysis

Accounted by the abovementioned validation, the XRD pattern of pure HA and PC/n-HA film were obtained, as shown in Fig. 4, which comprises the characteristic peaks of HA in the n-HA/PC film. Compared to pure n-HA, the peaks that emerge from the n-HA composite have marginal changes, but the tiny peaks due to n-HA in the film affirms its poorly crystallized apatite structure, which is similar to apatite in natural bone.[21,22]

The average crystal size was calculated[23] by Scherrer's equation (eqn (8))

$$D_{hkl} = \frac{k\lambda}{\beta_{hkl} \cos \theta} \quad (8)$$

where D_{hkl} is the average crystallite size, k is a constant related to the crystallite shape termed the shape factor (approx. equals unity), λ is the wavelength of X-ray radiation (1.54178 Å), β_{hkl} is the full width of the peak at half of the maximum intensity (rad), and θ is the Bragg angle. Based on Scherrer's equation, the average size of a HA crystal in the PC/n-HA film matrix was calculated using the diffraction peak at $2\theta = 27.73°$ (002) and $2\theta = 32.98°$ (300) of the XRD pattern to compare the products with each other. The resultant average crystal size was computed as nearly ≤20 nm. The shape of the n-HA crystal changed from lengthy columnar crystal to short columnar crystal, which is more similar to the ideal n-HA crystal structure. This result is consistent with the result of the SEM images. Jianguo *et al.*[9] posed a similar investigation of PC/n-HA composites by a solvent casted technique.

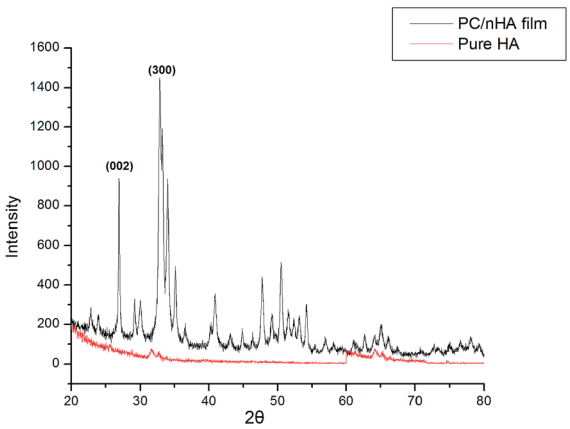

Fig. 4 XRD pattern of PC/n-HA film and pure HA.

3.3 Morphological studies

The inherent organic compatibility of n-HA poses an impediment to the molecular level adhesion between nano fillers and organic polymers. Thus, the most important requirements of molecular miscibility and homogeneity of the PC/n-HA was procured by a dynamic ultrasonication batch process, depicted by the FESEM micrograph. Fig. 5 correlates the surface morphology of pure n-HA and the PC/n-HA system with the spray coating mechanism. Fig. 5(a) illustrates the clustered needle pattern of pure n-HA filler. The n-HA crystals are on the nanometer scale and have a crystal size of 10–20 nm in diameter and 60–80 nm in length. The apatite crystals in natural hard tissues are usually thin-needle shaped, with a size of 5–20 nm by 60 nm and over 100 nm long in enamel.[9] The shape and size of

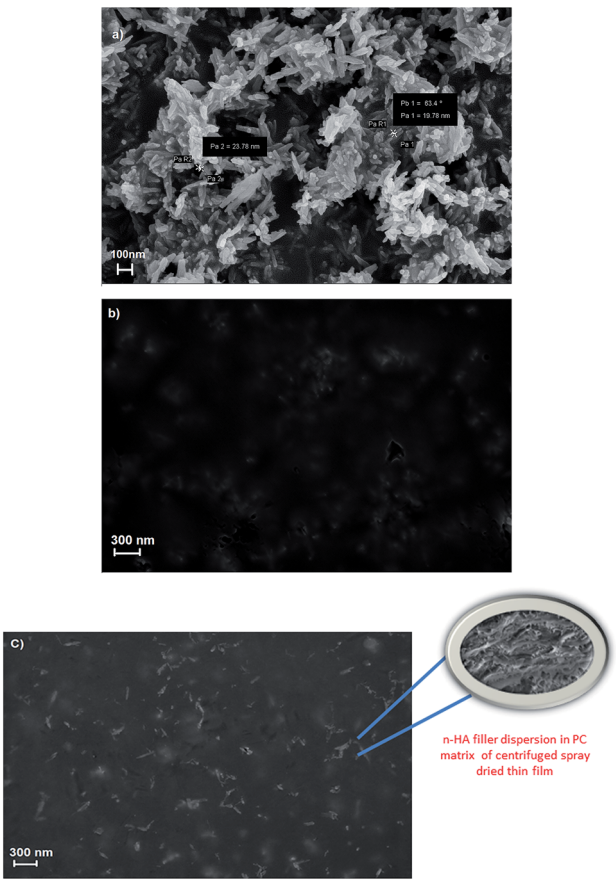

Fig. 5 (a) Pure n-HA, (b) morphology of spray gun dried PC/n-HA film, (c) morphology of centrifuged spray dried PC/n-HA film.

the prepared n-HA crystals were similar to those of the apatite crystals in natural bone, which was beneficial for preparing a biomimetic composite. The composite particles, as shown in Fig. 5(b) and (c), showed a size of 20–35 nm in diameter and 70–90 nm in length. A spray gun coated film indicates numerous asymmetric grain dispersed pattern that is randomly oriented compared to the centrifuged spray dried coated film that signifies symmetric distribution of n-HA fillers, confirming uniform oriented dispersion and molecular level adhesion between PC and n-HA.

3.4 Topographical and contact angle study

The topographical analysis of the PC/n-HA film from the spray gun and novel centrifuged spray practices majorly focuses on the surface roughness characteristics for bioengineering applications. The agglomeration of additives plays an important role in determining antibacterial behaviour of membranes. Enhancement in the agglomeration of additives can significantly mitigate the antibacterial properties of a substrate.[24] Fig. 6(a) shows the coarseness of the surface of the structure of n-HA filler over the PC matrix. The asymmetric and shortened spikes of n-HA were due to an agglomeration phenomenon during spray gun drying resulting in a surface roughness of 81.4 nm, whereas Fig. 6(b) emphasizes the uniform scaffold structure of n-HA embedded on a PC medium due to the perforated design of the spray disk on the centrifuged dryer, which ejects the droplets of PC/n-HA nanocomposite with higher jet impact on the slit for fine film formation with enhanced spikes and a surface roughness of 132 nm. The enhancement of surface roughness occurs due to an increased number of particles adhering to the glass, which enhances the amount of nanopillar formations over the surface, leading to increased roughness.[23] Fig. 6(c) shows the prominent cross-sectional view of the PC/n-HA surface, which affirms the encapsulative property of the nano HA symmetric distribution.

For hydrophobicity trait requirement for corrosion resistant application on titanium alloy and SS-316L biomedical grade screw coating, PC/n-HA plays a major role due to its delayed reaction functionalization to oxidation process in blood and bone interface.[25] Of all the sterilization techniques, grade 5 Ti alloy has been found to be the best at mitigating bacterial growth and showed the greatest promise as a more antibacterial implant material while simultaneously improving bioactivity.[26] As found in this study, the wettability of thin films produced by conventional method using centrifuged spray dyer upon spray gun film and the wettability change was consistent across the oxidation of TiO_2 surfaces, as shown previously by Wang *et al.*[27]

The oxidation of grade 5 Ti alloy can be described by the following reaction mechanism:

Oxidation of Ti alloy at points of stress in the crystal lattice:

$$2Ti(s) \rightarrow 2Ti^{2+}(aq) + 4e^{-}$$

Reduction of water at the site of rust due to O_2 in blood:

$$O_2(g) + 2H_2O(l) + 4e^{-} \rightarrow 4OH^{-}(aq)$$

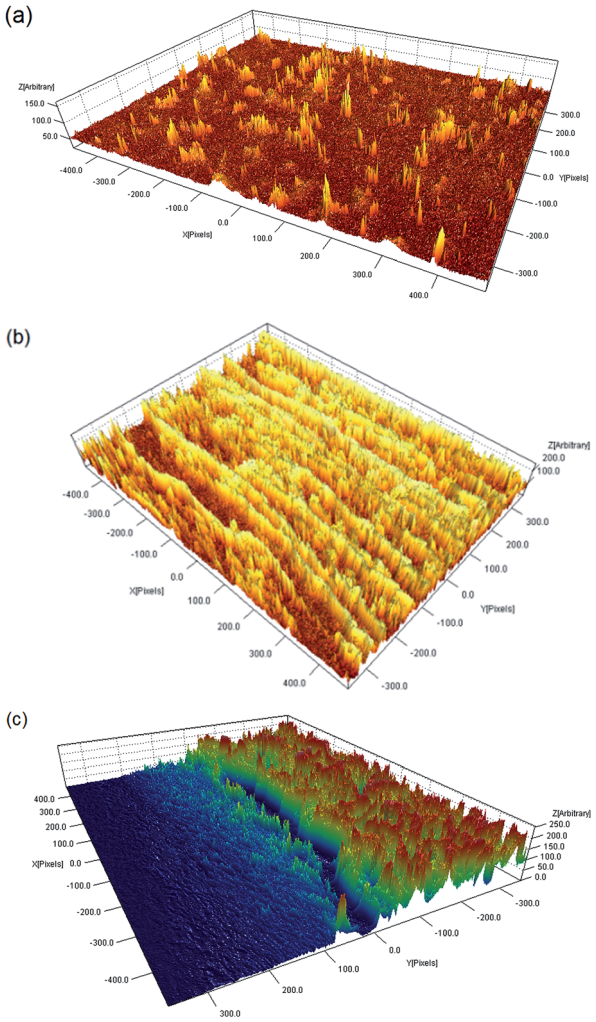

Fig. 6 Topographical analysis of PC/n-HA (a) spray gun dried film. (b) Centrifuged spray dried film. (c) Cross-sectional view of n-HA filler over PC matrix.

Overall equation:

$$2Ti(s) + O_2(g) + 2H_2O(l) \rightarrow 2Ti(OH)_2$$

Fig. 7(a) and (b) depict the contact angle analysis of the spray gun dried film, illustrating the 94.1° contact angle with 6.73 mm^2 of contact surface area, whereas the centrifuged spray dryer showed a significant spherical shape with contact angle of 131.7° and 2.19 mm^2 of contact surface area. Sahoo *et al.*[28] reported a similar contact angle study of a polystyrene–graphite composite by a spray coating technique, concluding with the hydrophobicity and lower wettability of the thin film. The types of contact angle that measure surface smoothness have been termed the advancing angle (θ_{ADV}) and receding angle (θ_{REC}).[29] If the water contact angle is less than 90°, the solid surface is considered hydrophilic, and if the water contact angle is greater than 90°, the solid surface is considered hydrophobic. A few

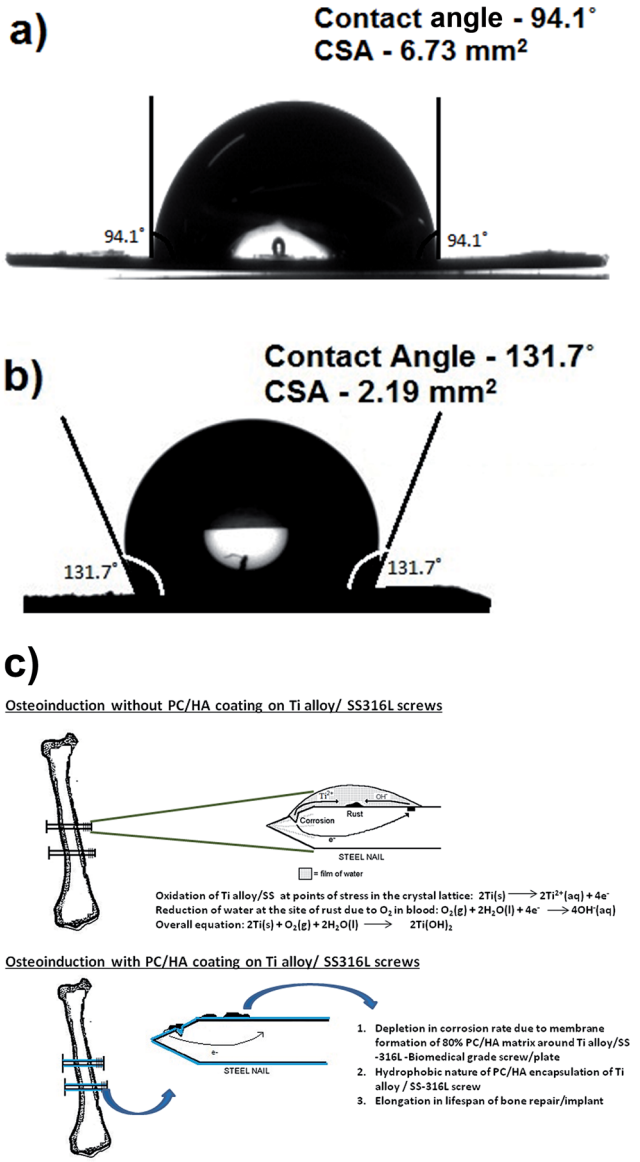

Fig. 7 Contact angle analysis of PC/n-HA (a) spray gun dried film (b) centrifuged spray dried film (c) application schematic.

materials with excessively rough surfaces may have a water contact angle even larger than 150°, due to the presence of air-filled pores under the liquid drop. These are called super-hydrophobic surfaces.[30] Thus, the surface can be expressed depending on the contact angle (θ) value as

- hydrophilic ($\theta < 90°$)
- hydrophobic ($\theta > 90°$)
- superhydrophilic ($\theta < 10°$)
- superhydrophobic ($\theta > 150°$)

Surface roughness and low adhesion energy are usually observed with a superhydrophobic surface. Wenzel proposed the term for the measurement of the contact angle of a liquid by considering a water droplet on a rough surface and homogeneous surface simultaneously and interpreted the concept that differs from the true contact angle (θ).

$$\cos(\theta_w) = R\cos\theta = R\frac{\gamma_{sv} - \gamma_{sl}}{\gamma_{lv}} \quad (9)$$

In eqn (9), R is the ratio of the actual area of the surface and the projected area. The wettability or non-wettability of a thin film depends on the roughness factor R that varies with the effect of surface chemistry on the true contact angle of the film.[31] The abovementioned phenomenon can be further elaborated by the Cassie–Baxter regime equation for the contact angle, given by

$$\cos\theta_{CB} = f_s\cos\theta + (1 - f_s) = f_s\left(\frac{\gamma_{sv} - \gamma_{sl}}{\gamma_{lv}} + 1\right) - 1 \quad (10)$$

where f_s is the fraction of the surface in contact with the liquid. $(1 - f_s)$ is the surface in contact with air allied with the interfacial energy of solid–liquid (γ_{sl}), solid–vapor (γ_{sv}) and liquid–vapor (γ_{lv}), θ_{CB} is the angle of contact for the Cassie–Baxter regime.

The contact angle can also be related to the work of adhesion *via* the Young–Dupré equation:

$$\gamma = (1 + \cos\theta) = \Delta W_{SLM} \quad (11)$$

where ΔW_{SLM} is the solid–liquid adhesion energy per unit area when in the medium M.

Eqn (10) and (11) exemplify the importance of surface roughness and adhesion energy in the measurement of the contact angle in quantifying a droplet touching the top of the thin film surface.[30] The hydrophobic nature of a surface can be ensured by the heightening of the contact angle due to air-filled pores present in large quantities at the solid surface. Hence, researchers concluded the effect of surface topology on the wetting property.[32]

The hydrophobic property of the PC/n-HA membrane reduces the corrosion rate and elongates the longevity of the bone implantation, depicted schematically in Fig. 7(c). Topographical and contact angle studies of two distinctive textures of PC/n-HA confirm that the short-peaked amorphous bed of grains causes the smoothened surface and minimal hydrophobicity of the spray gun dried film, whereas significant increment in spike height was observed with the centrifuged spray dried film with an enhanced contact angle of 131.7°. The results show that the n-HA fillers affect the coating surface energy and surface roughness, in turn influencing the wettability of the PC/n-HA coatings.

4. Conclusions

The perspective of newly developed process of employing a centrifuged spray dryer to produce a film coating has potential for large-scale economic applications for tailoring the nano-scale texture of a n-HA filler on a PC matrix. The PC/n-HA film epitomized uniform dispersion characteristics and hydrophobic affinity, from morphological and contact angle studies. The resultant roughness of 131 nm with hydrophobic behaviour (CA-131.7°) of the PC/n-HA film produced by the centrifuged spray dryer affirms that the topographical properties were

successfully modified for biomedical grade screw/plate coating application that have been very important for recent research practices. The centrifuged spray dryer design parameter aspects have been experimentally proposed for the velocity at the tip of the nozzle, $v_e = 38.03$ m s^{-1}, jet impact of spray, $F_x = 520.66$ N, and mass flow rate, 4.2×10^8 g cm^{-1} s^{-1}, as the average diameter of drop of solution is calculated as 48.28×10^{-7} m. The method permits faster and cheaper modification in the fabrication of coating materials with a higher specific surface area and similar or better capacity and cycle life compared with the materials prepared *via* conventional technologies. Thus, future theoretical studies gain interest over extensive studies, accumulating PC/n-HA spray drop trajectories, the heat transfer coefficient of an individual drop of a solution and the corresponding heat conduction/resistance property of a thin film, by the spray dryer technique, enhancing the suitability of novel spray dried film fabrication techniques for osteoinduction processes.

Acknowledgements

The authors acknowledge DIAT-DRDO Nano Project Program (EPIPR/1003883/M/01/908/2012/D R&D/1416 Dated: 28.03.2012), DRDO HQ, New Delhi for financial assistance. Mr Ramdayal Yadav and Mr Dhananjay Gunjal are acknowledged for continuous technical support and guidance. Authors would like to acknowledge DIAT COE Dr A. Kumaraswamyfor providing plagiarism check software 'turnitin' Copyright © 1998–2014 iParadigms, LLC) for this article. The authors would like to dedicate this paper to Prof. P. K. Khanna, Head, Department of Applied Chemistry, DIAT (DU), Pune.

Notes and references

1 M. R. Rogel, H. Qiu and G. A. Ameer, *J. Mater. Chem.*, 2008, **18**, 4233–4241.
2 M. Persson, G. S. Lorite, C. Sung-Woo, J. Tuukkanen and M. Skrifvars, *ACS Appl. Mater. Interfaces*, 2013, **5**, 6864–6872.
3 S. A. Hacking, M. Tanzer, E. J. Harvey, J. J. Krygier and J. D. Bobyn, *Clin. Orthop. Relat. Res.*, 2002, **405**, 24–38.
4 M. Sundfeldt, L. V. Carlsson, C. B. Johansson, P. Thomsen and C. Gretzer, *Acta Orthop.*, 2006, **77**(2), 177–197.
5 K. Hirakawa, J. J. Jacobs, R. Urban and T. Saito, *Clin. Orthop. Relat. Res.*, 2004, **420**, 10–17.
6 N. Katiyar and K. Balasubramanian, *RSC Adv.*, 2014, **4**, 47529–47535.
7 P. H. Kithva, L. Grøndahl, R. Kumar, D. Martin and M. Trau, *RSC Nanoscale*, 2009, **1**, 229–232.
8 D. Quan-Xiao, Q. Chen, W. Yang, Y. Zheng, X. Liu, L. Yuan-Li and Y. Ming-Bo, *J. Appl. Polym. Sci.*, 2008, **109**, 659–663.
9 L. Jianguo, Z. Li, Z. Yi, W. Huanan, L. Jidong, Z. Qin and L. Yubao, *J. Biomater. Appl.*, 2009, **24**(1), 31–45.
10 X. Liu and P. X. Ma, *Ann. Biomed. Eng.*, 2004, **32**, 477–486.
11 R. E. Treybal, *Mass Transfer Operations*, Mc Graw-Hill International Book Company, 3rd edn, 1980, pp. 695–697.
12 W. McCabe, J. Smith and P. Harriott, *Unit Operations of Chemical Engineering*, Mc Graw-Hill Chemical Engineering Series, 6th edn, 2000, pp. 362, 801–802.
13 T. Hobler, *Mass Transfer and Absorbers*, Pergamon Press, New York, 1966, pp. 469–471.
14 R. K. Bansal, *A Textbook of Fluid mechanics and Hydraulic machines*, L. Publication, 9th edn, 2010, pp. 797–98.
15 B. S. Banerjee, S. S. Khaira and K. Balasubramanian, *RSC Adv.*, 2014, **4**, 63380–63386.
16 E. M. Jacox, *J. Phys. Chem. Ref. Data*, 2003, **32**(1), 1–441.
17 J. L. Meyer and B. O. Fowler, *Inorg. Chem.*, 1982, **21**, 3029–3035.
18 Y. Li, *Macroscopic Approach and Microscopic Emulation-biomaterials Group Research*, University of Leiden, 1994, pp. 99–110.
19 Q. Liu, J. R. de Wijn, K. de Groot, A. Clemens and V. Blitterswijk, *Biomaterials*, 1998, **19**, 1067–1072.
20 X. Wang, Y. Li, J. Wei and K. de Groot, *Biomaterials*, 2002, **23**, 4787–4791.
21 G. Montel, G. Bonel, M. Heugheubaert, J. C. Trombe and C. Rey, *J. Cryst. Growth*, 1981, **53**, 74–99.
22 E. P. Pascalis, F. Betts, E. DiCarlo, R. Mendelsohn and A. L. Boskey, *Calcif. Tissue Int.*, 1997, **61**, 480–486.
23 B. N. Sahoo and K. Balasubramanian, *RSC Adv.*, 2014, **4**, 11331–11342.
24 R. Yadav and K. Balasubramanian, *Mater. Lett.*, 2013, **110**, 130–133.
25 K. L. Urish, MD, PhD; P. A. Anderson, MD; W. M. Mihalko, MD, PhD. and the AAOS Biomedical Engineering Committee, The Challenge of Corrosion in Orthopaedic Implants, April 2013, vol 7, no.4, AAOS Now (Research and Quality).
26 K. M. Kummer, E. N. Taylor, N. G. Durmas, K. M. Tarquinio, B. Ercan and T. J. Webster, *J. Biomed. Mater. Res., Part B*, 2013, **101B**(5), 677–688.
27 R. Wang, K. Hashimoto, A. Fujishima, M. Chikuni, E. Kojima, A. Kitamura, M. Shimohigoshi and T. Watanabe, *Nature*, 1997, **388**, 431–432.
28 B. N. Sahoo, B. Sabarish and K. Balasubramanian, *Prog. Org. Coat.*, 2014, **77**, 904–907.
29 L. Gao and T. J. McCarthy, *Langmuir*, 2006, **22**, 6234–6237.
30 W. A. Zisman and F. M. Fowkes, *Contact Angle, Wettability, and Adhesion*, ACS Publications, 1964, vol 43, pp. 1–51.
31 B. N. Sahoo and K. Balasubramanian, *RSC Adv.*, 2014, **4**, 22053–22093.
32 N. A. Patankar, *Langmuir*, 2003, **19**, 1249–1253.